Connective-tissue responses to defined biomaterial surfaces. I. Growth of rat fibroblast and bone marrow cell colonies on microgrooved substrates

John L. Ricci,[1] John C. Grew,[2] Harold Alexander[3]
[1]*Department of Biomaterials and Biomimetics, College of Dentistry, New York University, 335 East 24 Street, New York, New York 10003*
[2]*Department of Biology, New Jersey City University, 2039 Kennedy Boulevard, Jersey City, New Jersey 07305*
[3]*Orthogen Corporation, 505 Morris Avenue, Suite 104, Springfield, New Jersey 07081*

Received 3 March 2006; revised 24 December 2006; accepted 20 February 2007
Published online 9 August 2007 in Wiley InterScience (www.interscience.wiley.com). DOI: 10.1002/jbm.a.31379

Abstract: Surface microgeometry plays a role in tissue-implant surface interactions, but our understanding of its effects is incomplete. Substrate microgrooves strongly influence cells *in vitro*, as evidenced by contact guidance and cell alignment. We studied "dot" colonies of primary fibroblasts and bone marrow cells that were grown on titanium-coated, microgrooved polystyrene surfaces that we designed and produced. Rat tendon fibroblast and rat bone marrow colony growth and migration varied ($p < 0.01$) by microgroove dimension and slightly by cell type. We observed profoundly altered morphologies, reduced growth rates, and directional growth in colonies grown on microgrooved substrates, when compared with colonies grown on flat, control surfaces ($p < 0.01$). The cells in our colonies grown on microgrooved surfaces were well aligned and elongated in the direction parallel to the grooves and colonies. Our "dot" colony is an easily reproduced, easily measured and artificial explant model of tissue-implant interactions that better approximates *in vivo* implant responses than culturing isolated cells on biomaterials. Our results correlate well with *in vivo* studies of titanium dioxide-coated polystyrene, titanium, and titanium alloy implants with controlled microgeometries. Microgrooves and other surface features appear to directionally or spatially organize cells and matrix molecules in ways that contribute to improved stabilization and osseointegration of implants. © 2007 Wiley Periodicals, Inc. J Biomed Mater Res 85A: 313–325, 2008

Key words: microgroove; *in vitro*; cell-surface interactions; fibroblasts; bone marrow

INTRODUCTION

More than 325,000 hip arthroplasties, 325,000 knee replacements,[1] and 350,000 dental implants[2] are performed in the United States alone each year. As these figures increase over the upcoming decades, implant designs that result in better clinical applications of these devices will be significant medically and beneficial economically. Many factors contribute to the body's responses to biomaterial implants, including the composition, surface chemistry, geometry, and surface texture of the implant, along with various types of cells and molecules that the body provides. By improving our understanding of the biology of the tissue-implant interface, we will contribute to design improvements that will maximize the clinical success of these implanted devices.

Correspondence to: J.C. Grew; e-mail: JGrew@NJCU.edu

© 2007 Wiley Periodicals, Inc.

Tissue responses to implant surfaces

A lengthy history of orthopedic implant loosening led manufacturers to undertake various surface treatments to improve implant stability and integration.[3–8] Surface microgeometry plays a role in tissue-implant surface interactions, although well-defined causal relationships are not yet established. In brief, smooth implant surfaces tend to develop thick fibrous encapsulation, which impairs implant assimilation. Roughened implant surfaces tend to develop more extensive bony integration, which stabilizes implants. In general, bone-forming cells adhere better to complex surfaces, while fibroblasts prefer smooth surfaces.[9–22]

In vivo, grooved and machined metallic and polymeric surfaces appear to orient cells and matrix molecules in a fashion that is dependent on groove depth.[23–35] Microgrooves modulate the growth of epithelial cells, depending on their orientation.[36–41] Surface texturing also affects other processes that

may stabilize the implant-tissue interface[41,42] or influence the inflammatory and immune responses to implanted devices.[43–46]

Titanium dioxide-coated polystyrene, titanium alloy and commercially pure titanium wafer, and intramedullary-rod implants bearing controlled microgrooves enhanced the formation of organized bone tissue and promote the overall tissue integration of these devices *in vivo*.[37,47] Electron microscopic results suggested that these surfaces orientated cells, extracellular matrix, and bone trabeculae. Roughened and polished surfaces of the same types showed moderate, nondirectional bone formation, and nontextured surfaces showed mostly fibrous encapsulation.[48,49]

The position and orientation of microgrooves might be employed to better accommodate the mechanical forces bearing on the tissue-implant interface by reducing shear and inflammation, and by modulating the growth of various cell and tissue types.[13,50–53] Some evidence indicates that surface texture influences cell responses to biological mediators and differentiation patterns.[54,55]

Microgeometry

We designed, produced, and employed cell culture substrates that each bear microgrooved and flat, control areas. Our substrates were prepared with square-wave microgrooves, which most strongly affect cellular contact guidance phenomena.[30,56] Our experimental substrates have microgroove periodicities that range from 3.55 to 23.75 μm. Periodicity, also called repeat spacing or pitch,[26] is the distance comprising one groove and one ridge of uniform dimension, and is represented by $a + b$, in Figure 1. Thus, our substrates had microgroove widths in the 2–12 μm range, which yield the greatest contact guidance effects in connective tissue and epithelial cells, on cell colony growth and migration.[37,57–59] This model was developed to characterize the most basic implant colonization events. Moreover, our model enables us to relate observations of individual cells grown on similar surfaces *in vitro* and *in situ* tissue responses.

Our methodology enables us to easily and economically produce polystyrene substrates bearing three-dimensional microgrooved surfaces. Many investigators have employed gold-alkyl thiol self-assembling monolayer (SAM) or microcontact printing/microlithography techniques to produce two-dimensional substrates with micropatterned attachment-promoting or -inhibiting proteins and other substances[60–63] [for review, see Whitesides et al., (2001)[64]]. These substrates elegantly modulate the distributions, sizes, shapes, differentiation, growth, and mitotic and apoptotic fates of a variety of cell types

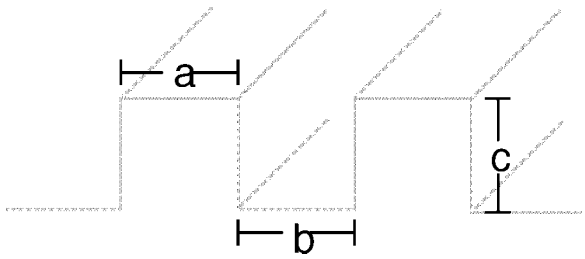

Figure 1. Diagram of square-wave microgroove features.

in vitro,[46,60,65–69] including nerve[70,71] and muscle.[72–74] However, the two-dimensionality of micropatterned surfaces make it difficult to envision their widespread clinical implementation, and *in vivo* studies of micropatterned surfaces are lacking.

Evidence indicates that molded, polymer substrates that bear micrometric features comparable in size to cells appear to have the most profound effects on cell morphology and behaviors. These effects appear to depend on microgroove shape and depth, as well as width.[23,35,40,48,49,57,58,75–83] These investigations are descended from initial studies of the effects of macrogeometric and mesogeometric surface features on orthopedic implants and implant materials.[26,84] Substrate features considerably smaller than cells have less pronounced effects on cell morphology and behavior.[23,56] The *in vitro* effects of implant texturing on individual cells are evaluated in a companion report.[85]

Surface microgeometry effects on tissue responses appear to supercede and outlast those because of other factors. Studies of vascular, dental, and orthopedic implant materials reveal that small variations in composition and surface chemistry invoke minimal changes in cell and tissue responses, while modifications of surface microgeometry exert stronger influences on cell behavior.[16,86–88] For instance, the robust cell attachment and growth induced by materials with high surface free energies *in vitro*[89,90] are lost in the presence of serum proteins.[89,91–93] Surface chemistry and surface energy may influence the types, distributions, configurations, and turnover of proteins on an implant surface[94] and immune responses to implants further complicate this system.[95]

Dot culture model and assays

We employed a novel combination of physical substrate features and an artificial tissue matrix to examine contact guidance in colonies of connective tissue cells. Our cell colony system spans the gap in understanding between observations of individual cells on similar surfaces and examinations of tissue responses to implants *in vivo*. These events model the early stages of a wound healing or foreign-body

(i.e., implant) response. Our unique system is an artificial explant model that examines the initial events of colonies of primary cells as they colonize substrates while contained within an artificial extracellular matrix. An extensive review of the literature revealed numerous reports of cellular and tissue-level responses to culture substrates, but no reports that examine the responses of cell colonies to complex growth substrates. Our model is unique because it enables us to examine cell-surface interactions in a system where three-dimensional substrate features are controlled and the composition of the surrounding, three-dimensional collagenous matrix is controlled. As such, the cells we observed were simultaneously influenced by permanent, physical substrate features such as those that might be present on an implanted device, and by three-dimensional cell-signaling events initiated by the interaction of membranous integrins and other cell-adhesion molecules with the enveloping matrix gel. These conditions create a more "natural" milieu for the cells we studied. We herein document the effects of surface microgrooves on cell colony growth *in vitro*, using a collagenous matrix and two cell types that are relevant to the application of orthopedic implants.

We measured the growth of colonies of fibroblastic and osteogenic cells on microgrooved substrates in a controlled environment. The surface areas covered by rat tendon fibroblast (RTF) and bone marrow (RBM) colonies grown on microgrooved substrates reveal how the microgrooves affected the rate of growth of the colonies, while the aspect ratios of the colonies indicate how the microgrooves affect the direction of colony growth. We employed primary cultures of RTF and RBM cells within the first three passages throughout our studies. It is important to study cells that are not extensively differentiated from their *in vivo* state to draw meaningful conclusions from their observed behaviors. Therefore, these cells are as phenotypically similar to their *in vivo* equivalents as any that can be obtained.

Consistent RTF and RBM colony growth is established by day 3 in culture, and control colony diameters increase in a linear fashion through day 12. Thus, we measured RTF and RBM colonies at 4 and 8 days to document the most consistent period of colony growth. To eliminate small variations in initial colony size and shape that result from the influences of the different microgroove dimensions on the shapes of the liquid collagen drops as sources of error, we calculated and report increases in colony length, width, and area between 4 and 8 days.

Rationale

We produced a simplified model of a connective tissue growing on substrates that are known to modify the growth, distribution, and properties of those tissues. With this model, we quantitated, characterized, and compared those effects. We are also able to clarify the cell- and tissue-level responses to implant surface microgrooves that we have observed *in vivo*. Overall, we intend to apply this information to create implant surface designs that control tissue responses at implant surfaces to specific microgeometric designs. These designs will shift the tissue response to these implants away from fibrous encapsulation and toward bone integration. This development will be of significant clinical value.

MATERIALS AND METHODS

Cell culture substrate fabrication

We molded polystyrene substrates from silicon-wafer templates that were precision-fabricated at the National Nanofabrication Facility at Cornell University for these experiments. Microgrooved silicon-wafer templates were fabricated by microlithography. Template designs having parallel microgrooves were created with the computer-aided design program Symbad. These designs were transferred to a GCA Optical Pattern Generator to fabricate photomasks. Three-inch silicon wafers were coated with a 15-μm layer of silicon dioxide on an IPE Chemical Deposition System. The wafers were placed on a GCA Projection Mask Aligner and a photoresist layer was applied. Square-wave microgrooves were created by multiple reactive-ion etching (RIE) techniques on magnetron ion etcher (MCR). The templates were afterwards placed on an IPC Barrel Etcher to strip the photoresist. The bare silicon surfaces were further etched within a Plasma Therm RIE System. The finished templates were washed in hydrochloric acid and attached to 3-inch aluminum rods to provide rigidity. An example mold surface is shown in Figure 2.

Cell culture substrates were created from the silicon templates by solvent-casting. The casting solution consisted of 15 g of polystyrene cell-culture dish (Corning) fragments dissolved in 100 mL ethyl acetate. A dam was fashioned from tape around each mold, onto which the casting solution was poured. 8 mm of casting solution produced 0.5 mm-thick polystyrene replicates when placed under high vacuum for 24 h to eliminate bubbles and to evaporate the ethyl acetate solvent. After water wash, the replicates were peeled from their respective templates and cut into 50 mm circles to yield the cell culture substrates evaluated in our studies. The substrates were air-dried for at least 24 h to completely evaporate the solvent. They were then coated with a 60 nm titanium oxide layer in a Denton Vacuum Evaporator. The efficiency and consistency of this coating procedure and the surface chemistry of cross-sections of the coated substrates was verified with a Fisons-Kevex EDAX system installed on a JEOL JSM T300 SEM to measure Ti and employed a light-element detector to measure O. The substrates were affixed within 60-mm petri dishes with a heated probe, and ethanol-sterilized.

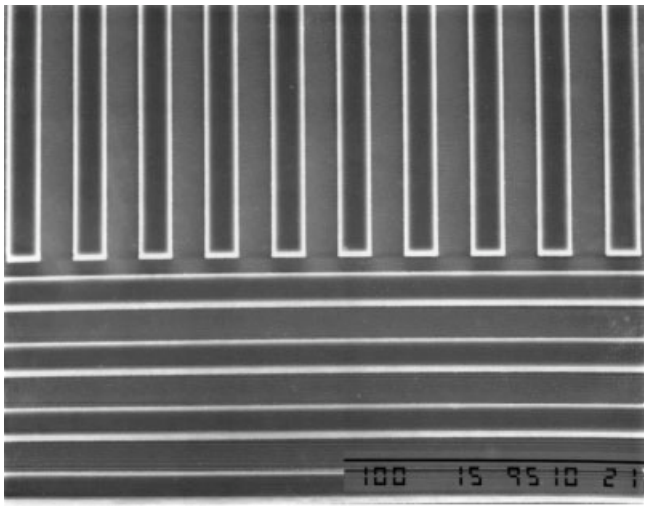

Figure 2. Scanning electron micrograph of a portion of a silicon-wafer mold bearing 12-μm microgrooves. The image shows the intersection of areas bearing microgrooves that intersect at a right angle. Bar = 100 μm.

Analysis of experimental substrate surfaces

The dimensions of the substrate square-wave surface microgeometries were measured with a workstation consisting of a Leitz Orthoplan transmission light microscope or Wild MC3 stereomicroscope, an MTI video camera, an Apple Macintosh computer with Perceptics video acquisition hardware, and Scientific Imaging Solutions Workstation TCL-Image image processing/image analysis software. The dimensions of the microgrooves determined by light microscopy were used to calibrate a JEOL JSM T300 scanning electron microscope (SEM). The groove depths were determined by comparing photomicrographs of the surfaces at 0° and 45° tilt angles.

Preparation of RTF cultures

RTF cultures were initiated from explanted hindfoot extensor tendons that had been removed from male, 14-day-old Sprague-Dawley rats (Charles River Laboratories) sacrificed by Halothane overdose. This painless method of sacrifice does not contaminate the tendon tissue. Four extensor tendons were removed from each foot and placed in Hank's balanced salt solution (HBSS) containing 1% penicillin–streptomycin solution. Tendons were then separated from sheath tissue by microdissection and used to establish explant cultures. The tendon explants were discarded after 12–17 days and the adherent cells were subcultured. The cultures were treated with a 0.25% trypsin solution in calcium- and magnesium-free HBSS for 20 min, rinsed in medium containing 10% fetal bovine serum, and counted with a hemacytometer. RTF cells obtained this way were used to inoculate additional culture plates or to initiate dot cultures (see below).

All cultures were grown in a 37°C incubator in a humidified atmosphere containing 5% CO_2, and maintained with Dulbecco's Modified Eagle's Medium (DMEM) at pH 7.4 containing 10% fetal bovine serum, 1% penicillin–streptomycin solution, and 50 mg/mL ascorbate to stimulate matrix synthesis. All dissection and culture procedures were conducted under sterile conditions with reagents obtained from GIBCO/Invitrogen.

Preparation of RBM cultures

RBM cultures were prepared from 14-day-old rat femurs according to the method of Maniatopoulos et al.[96] In brief, femurs were dissected from rats euthenized in the manner described earlier. The ends of each femur were cut off, the marrow cavity was flushed with a syringe containing supplemented DMEM, and the expelled marrow tissue was dispersed by repeated passage through the syringe needle and incubated in a culture plate. This type of bone marrow preparation self-segregates into its attachment-dependent stromal cells and its hemopoietic elements, which do not attach to a substrate. After 24 h, the unattached elements and undispersed marrow tissue were removed, and the remaining attached cells were then allowed to grow to confluency. All dissection and culture procedures were conducted under sterile conditions with the reagents described earlier, except that DMEM was supplemented with 15% fetal bovine serum.

Establishment of RTF and RBM "dot" colonies

RTF and RBM colonies were established by embedding RTF and RBM cells in a collagenous matrix. To insure that the cells retained their *in vivo* behavioral characteristics, only first-, second-, and third-passage cultures were used in these experiments. RTF and RBM cell suspensions were mixed with HCl-solubilized, bovine type I collagen solution (Collagen Corporation) to create these colonies. A 0.3 mg collagen/mL solution at pH 3 was mixed with cells in 10× DMEM containing NaOH while kept on ice, and subsequently dispensed as 2 μL aliquots containing 20,000 cells each onto the control and microgrooved substrates. The cell–matrix mixture thereafter polymerized upon warming to form dot colonies in the incubator atmosphere. These initial colonies were about 2 mm in diameter (Fig. 3), but varied according to the dimensions of the underlying microgroove dimensions.

Measurement of RTF and RBM colony growth

Collagen-gel dots containing RTF and RBM cells acted as sources of cells for colony formation. Colonies were grown on substrates bearing 1.75, 3.50, 6.33, 7.75, or 11.75 μm-wide grooves and comparably sized ridges, as well as flat, control areas of the same substrates. RTF and RBM cells from the same animals were used to initiate groups of 5–8 colonies per substrate type in separate culture dishes. Four colonies each were initiated on the flat control and experimental sides of each 50 mm-diameter substrate fitted within a 60-mm culture plate. Thus, we initiated 40–64 colonies of each cell type on the control and microgrooved areas of each type of substrate. The cultures were

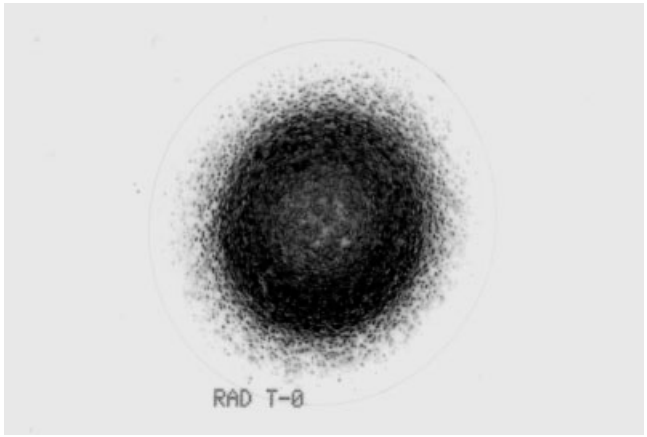

Figure 3. Negative image of a light micrograph of an RTF "dot" colony newly established on a control substrate. The cells are evident within a halo of collagen gel. The colony is ~2 mm in diameter. Original magnification = ×10.

maintained under standard sterile conditions in appropriate media, as described earlier.

RTF and RBM cultures were fixed in 10% phosphate-buffered formalin and stained with toluidine blue after 4 and 8 days. Cultures were examined and representative colonies were photographed using light microscopy with the imaging system described earlier. Images of the colonies were digitized and measured to quantify colony outgrowth characteristics. The lengths (i.e., parallel to surface microgrooves, in mm), widths (i.e., perpendicular to surface microgrooves, in mm), aspect ratios (length-to-width ratios), and areas (in mm^2) were determined for colonies growing on each control and microgrooved surface. Increases in colony length, width, and area between days 4 and 8 were determined by subtracting day 4 values from corresponding day 8 values. Aspect ratios were calculated for all colonies on days 4 and 8.

Data analysis and statistics

Data was recorded in MicroSoft Excel spreadsheets for statistical analysis. The mean (μ), standard deviation (SD), and sample size (n) were calculated for each group (i.e., microgroove dimension). The means of all groups within an experiment were compared by one-way analysis of variance (ANOVA). The means of individual groups were compared directly with Student's t-test (2-tailed, unpaired) for nonparametric data. Aspect ratio data for 4- and 8-day colonies grown on each microgroove substrate type was compared with Student's t-test (2-tailed, unpaired) for nonparametric data. Graphs were prepared from the data spreadsheets with KaleidaGraph (Synergy Software). Group means, with corresponding SD and n values are indicated, as are levels of statistical significance, if any. In each graph, the level of statistical significance for the mean of each group versus any other group mean(s) is indicated by the presence of the contrasting group name in standard type (i.e, C, 2, 6, 8, or 12) for p-values <0.05 and in boldface type for p-values < 0.01 (i.e, **C**, **2**, **6**, **8**, or **12**).

TABLE I
Measured Dimensions of the Substrate Square-Wave Microgrooves

Template Name	Microgroove Dimensions ($a \times b \times c$)	Microgroove Periodicity
2	$1.80 \times 1.75 \times 1.75\ \mu m^3$	3.55 μm
4	$3.50 \times 3.50 \times 3.50\ \mu m^3$	7.00 μm
6	$6.50 \times 6.33 \times 5.00\ \mu m^3$	12.83 μm
8	$8.00 \times 7.75 \times 7.50\ \mu m^3$	15.75 μm
12	$12.00 \times 11.75 \times 7.50\ \mu m^3$	23.75 μm

RESULTS

Production of microgrooved silicon wafer molds and polystyrene substrates

Table I summarizes the dimensions of the microgroove features of our culture substrates. Note that the maximum depth attained by our procedure was 7.50 μm, and that templates with 12-μm grooves had rectangular shapes. An example of a microgrooved, polystyrene cell culture substrate is shown in Figure 4.

RTF and RBM colony growth on microgrooved and control substrates

Our experimental design revealed significant variance, as measured by one-way ANOVA, among mean group values of RTF and RBM colony length and width changes, area increases, and aspect ratios at 4 and 8 days. In all cases except colony area increase on 2-μm grooves, the confidence levels for determining statistical significance (p-value) were 99% or greater (i.e., $p \leq 0.01$); in many cases our results carried extremely high significance levels (i.e., $p \leq 10^{-25}$).

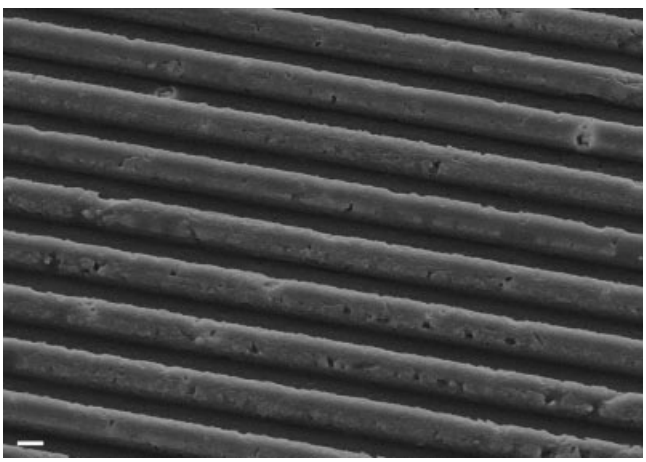

Figure 4. Scanning electron micrograph of a portion of a polystyrene cell culture substrate bearing 12-μm microgrooves. Bar = 10 μm.

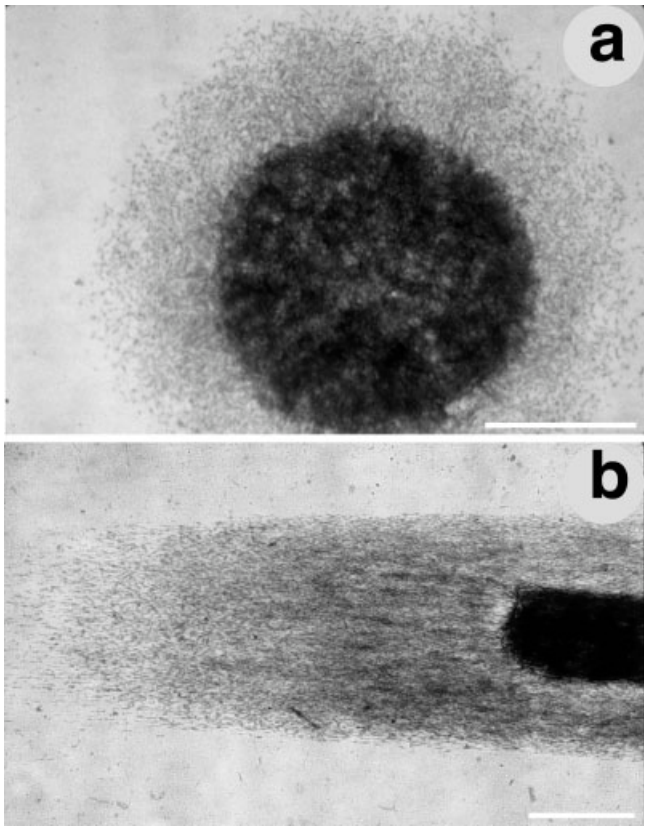

Figure 5. Light micrograph of RTF colonies grown for 4 days on control and 6-μm microgrooved substrates. The colony grown on the control substrate (a) displays radial outgrowth from the initial collagen gel "dot" seen as the dark area in the center of the colony. The extent of colony outgrowth can also be seen. The original gel dot is ~2 mm in diameter. The colony grown on the 6-μm microgrooved substrate (b) displays extensive outgrowth from the initial gel dot in the direction parallel with the direction of the microgrooves. Less extensive outgrowth is observed in the direction perpendicular to the direction of the microgrooves. This microgroove dimension is below the resolution limit of the microscope at this magnification. Bar = 1 mm (a and b).

Both RTF and RBM colonies grew consistently from day 4 through day 8 on control and microgrooved substrates. Colony outgrowth occurred in a radial fashion on control substrates, with colonies consistently increasing in diameter. Colony outgrowth on microgrooved substrates occurred in a nonuniform, directional fashion, with colonies consistently exhibiting significantly increased growth in parallel with the direction of the microgrooves and significantly reduced growth perpendicular to the direction of the microgrooves (Figs. 5–7), when compared with control colony diameters. Moreover, cells at the growing edges of the colonies cultured on control substrates were randomly oriented, while cells at the growing edges of the colonies cultured on microgrooved substrates were directionally oriented in parallel with the surface microgrooves. (Figs. 8 and 9).

The combined effects of the enhancement of RTF and RBM colony growth in the direction parallel to the direction of underlying microgrooves and the impairment of colony growth in the direction perpendicular to the direction of the microgrooves caused the colonies to assume ovoid shapes, with aspect ratios greater than 1. Colonies grown on control substrates were circular and had aspect ratios equal to 1. Except for RTF colonies grown on 2 μm grooves, the colonies became more eccentrically shaped with time. However, colony aspect ratios at 8 days were significantly increased over colony aspect ratios at 4 days only in RTF cells grown on 6- and 8-μm grooves ($p < 0.05$ and $p < 0.01$, respectively) and in RBM cells grown on 4- and 6-μm grooves ($p < 0.01$). While there was an evident correlation between colony elongation with microgroove width, this trend did not extend beyond 8 μm grooves; there was no increase in colony aspect ratios in colonies grown on 12 μm grooves when compared with colonies grown on 8 μm grooves. Mean colony aspect ratios for RTF and RBM colonies grown on microgrooved substrates are reported in Figure 10.

Substrate microgrooving significantly impaired increases in RTF and RBM colony area between 4 and 8 days (Fig. 11). The measured areas represent colony formation as projected on the surface area of the substrates, and does not attempt to include areas of cell and colony attachment occurring on the walls of the microgrooves. Overall, microgrooved surfaces have areas that are up to twice the area of a flat surface.

DISCUSSION

Substrate microgeometry

Our fabrication method provided us with an inexpensive, reproducible protocol for producing a supply of microgrooved cell culture substrates. Minor defects were observed on the polystyrene replicates (Fig. 4), typically small cavities and fissures, which represent a secondary level of featuring on the cell culture substrates. The cumulative effects of these defects did not appear to affect the primary effects of the microgrooves (i.e., cell alignment, directional colony growth, reduced colony area), and probably served to improve the overall adherence of the cells and colonies to the substrates.

Our substrates were vapor-deposited with titanium oxide to create hydrophilic surfaces that supported cell attachment and growth on molded polystyrene.[97] This surface simulates that of a

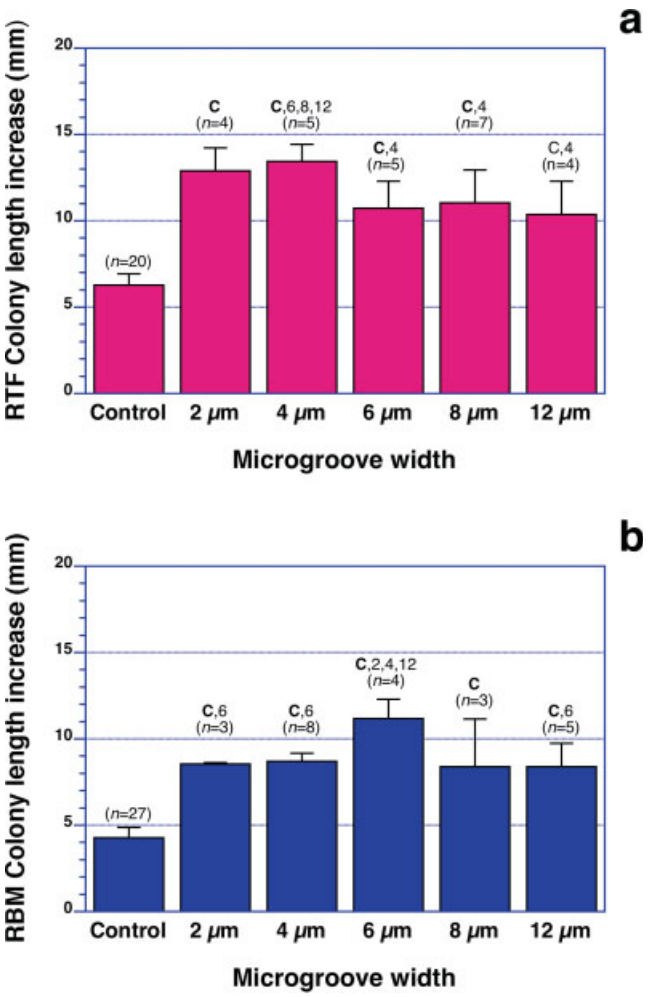

Figure 6. Graphs comparing mean increases, between days 4 and 8, in the lengths of RTF and RBM colonies grown on microgrooved substrates and in the diameters of RTF (a) and RBM (b) colonies grown on control substrates. Notations report SD, sample size, and levels of statistical significance in all graphs, as described earlier. [Color figure can be viewed in the online issue, which is available at www.interscience.wiley.com.]

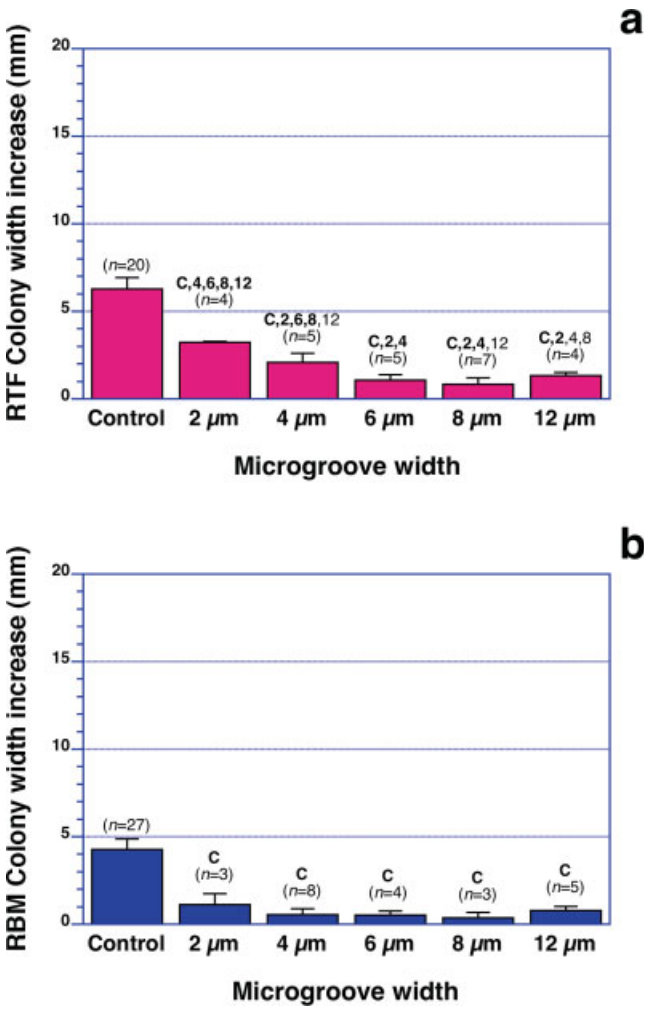

Figure 7. Graphs comparing mean increases, between days 4 and 8, in the widths of RTF (a) and RBM (b) colonies grown on microgrooved substrates and in the diameters of RTF and RBM colonies grown on control substrates. [Color figure can be viewed in the online issue, which is available at www.interscience.wiley.com.]

titanium or titanium alloy implant. Titanium oxide becomes complex, heterogeneous, and hydroxylated under physiologic and *in vitro* conditions[98]; adsorbs lipoproteins, glycolipids, proteoglycans, and collagens[99]; stimulates integrin-mediated cell signaling[100]; and dramatically improves the wetability of microgrooved polymers.[43]

"Dot" culture model

Our experimental design demonstrated the formation and growth of both RTF and RBM cell colonies on a variety of substrates, although RBM cells required higher serum levels and grew at a slower rate than RTF cells. Our dot culture system is a novel, artificial explant model with which we demonstrated significant alteration of the behavior of connective-tissue cells grown within an artificial extracellular matrix. This unique approach enabled us to evaluate the responses of cells that typically exist within such a three-dimensional matrix while surrounded by matrix proteins, wherein they are much more likely to behave as they would *in situ* at a site of wound healing or implant placement. Each cell that is contained in a three-dimensional gel of matrix proteins interacts with matrix molecules across its entire surface, and is expected to have a fully formed cytoskeleton and to behave more typically than a cell seeded on to any surface. Moreover, cells suspended within an artificial matrix would interact in a way that is more similar to cells within a tissue than would cells cultured on a flat surface. As such, previous studies that omit the important influences of encapsulating matrix molecules on

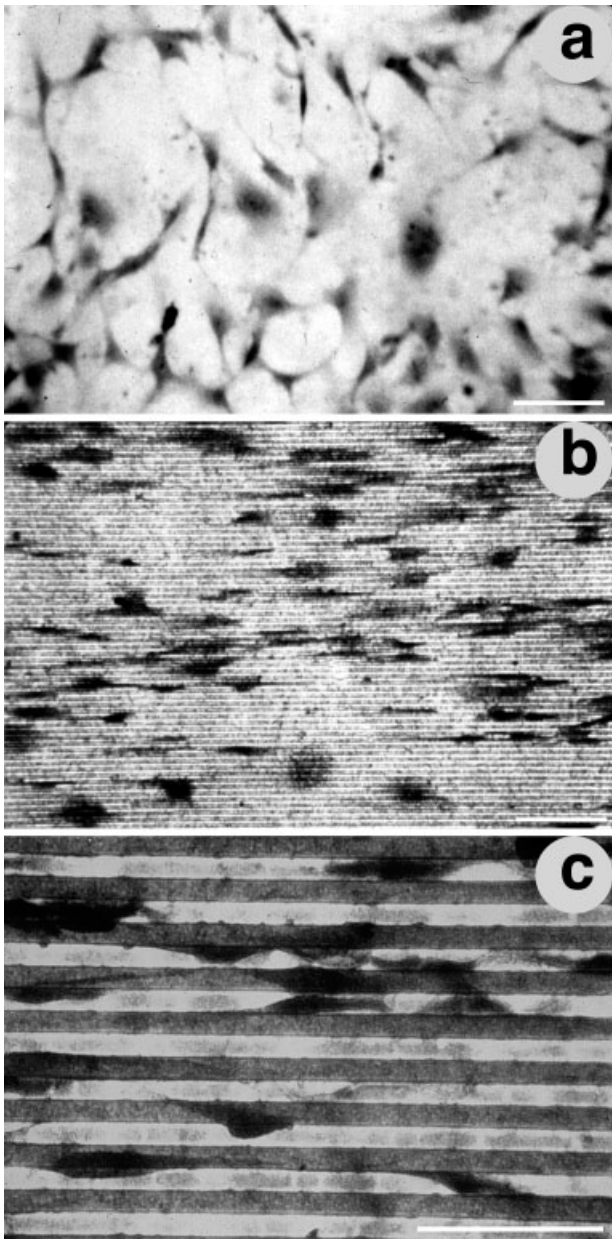

Figure 8. Light micrographs of RTF cells from colonies grown on control (a), 4-μm microgrooved (b), and 12-μm microgrooved (c) substrates for 4 days. Cells from the colony grown on the control substrate display random orientations and are well spread. Cells from the colony grown on the microgrooved substrate are attached to the tops, bottoms, and sides of the microgrooves, are aligned with the direction of the microgrooves, and are elongated. Cells grown on the 4-μm microgrooved substrate are frequently seen spanning several grooves and ridges each, while cells grown on the 12-μm microgrooved substrate are situated atop the ridges or within the grooves. Bar = 100 μm (a, b, and c).

cultured cells provide an incomplete description of the responses of those cells to microgrooves and other surface treatments, and of the potential application of those surface treatments in biomedical device design.

While explant cultures can be used to measure cell colony formation on surfaces[101] they tend to form irregular colonies that cannot be easily analyzed, because of variations in shape, cell number, and area of contact with the substrate. Dot cultures are initially circular, consist of a uniform number of cells bound together within a collagenous gel, and demonstrate an easily reproduced and measured pattern of growth. The consistency and measurability of our model makes it appropriate for the present studies, the results of which better explain *in vivo* observations than do studies of isolated cells grown directly on simulated biomaterials.[47–49]

Effects of microgrooves on RTF and RBM colony growth

RTF and RBM cell colonies consistently demonstrated differential growth tendencies when cultured on microgrooved substrates. All colonies elongated

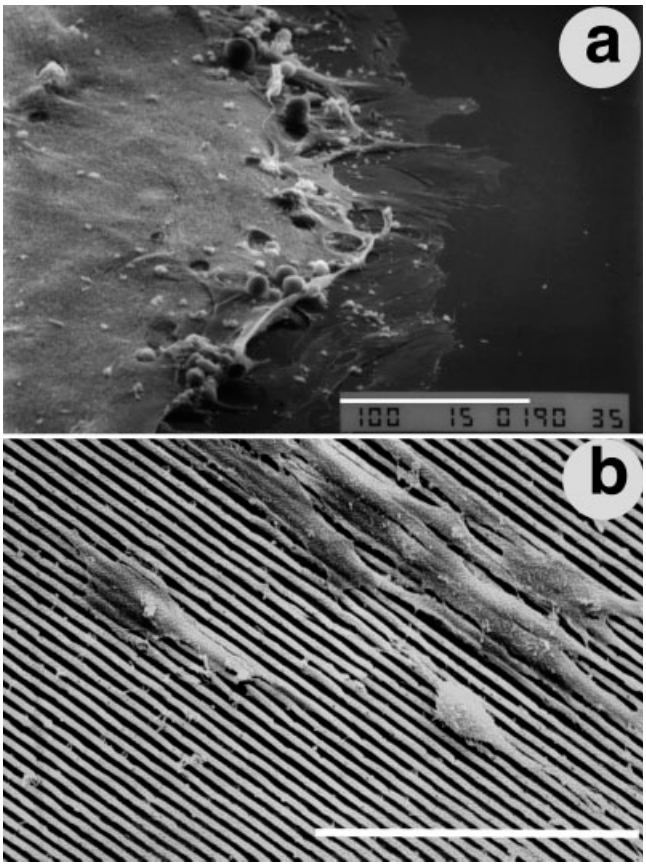

Figure 9. Scanning electron micrographs of an RTF cell colony grown on a control substrate (a) and of individual RTF cells from a colony grown on a 2-μm microgrooved (b) substrate. RTF cells are seen emerging from the edge of the control colony. Those cells are well spread and randomly orientated, while cells grown on the microgrooved substrate are profoundly elongated in the direction of the microgrooves. Cells within the control colony are enmeshed in collagen, while those near the colony's edge are frequently rounded, a shape associated with cell division. Bar = 100 μm (a and b).

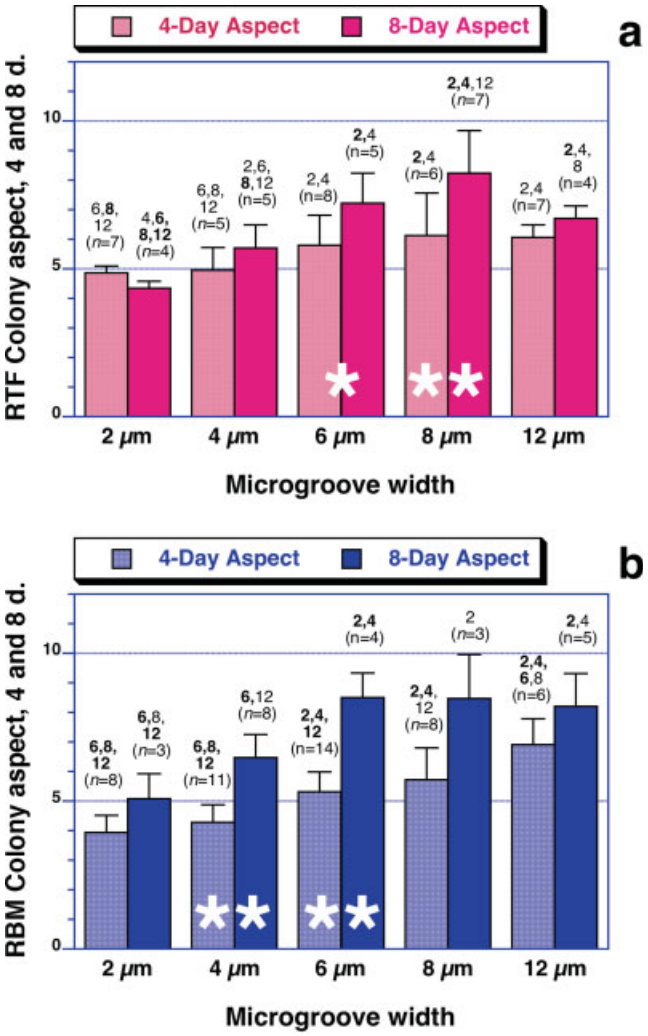

Figure 10. Mean colony aspect ratios for RTF (a) and RBM (b) colonies grown on microgrooved substrates for 4 and 8 days. A general trend of colony elongation over time on microgrooves up to 8 μm is evident. Significant increases between the mean aspect ratios of colonies grown on microgrooved surfaces for 4 versus 8 days are indicated by single and double asterisks ($p < 0.05$ and $p < 0.01$, respectively). The aspect ratios of control colonies are 1 (not shown). [Color figure can be viewed in the online issue, which is available at www.interscience.wiley.com.]

in the direction parallel to those of the microgrooves to a greater degree than colonies grown on flat substrates increased in diameter ($p \leq 0.01$). Conversely, all colonies elongated in the direction perpendicular to those of the microgrooves to a lesser degree than colonies grown on flat substrates increased in diameter ($p \leq 0.01$). The overall result of these growth alterations was that colony formation on microgrooved substrates resulted in elongated colonies having aspect ratios exceeding 1, while colonies grown on flat surfaces remained circular.

RTF and RBM colony growth and migration varied significantly by microgroove dimension and varied slightly by cell type. The microgrooved surfaces yielded elongated colonies that contained cells that were oriented in the direction parallel to the microgrooves and the long axes of the colonies. This orientation caused the cells to be "channeled" along the microgrooves, when compared with control cultures, wherein the outgrowing cells moved randomly across the flat surfaces. The 6-, 8-, and 12-μm microgrooves appeared to "channel" the cells most efficiently. Both cell types attached to and oriented themselves with the grooves and along the flat tops of the elevated ridges of these microgrooves. This resulted in enhanced longitudinal growth and impaired horizontal growth by both cell types on these surfaces. This colony elongation may have been partly due to differential degrees of contraction by the gel after initial deposition. However, our final observations are principally the effects of differential growth and migration of cells well beyond the boundaries of the initial dots.

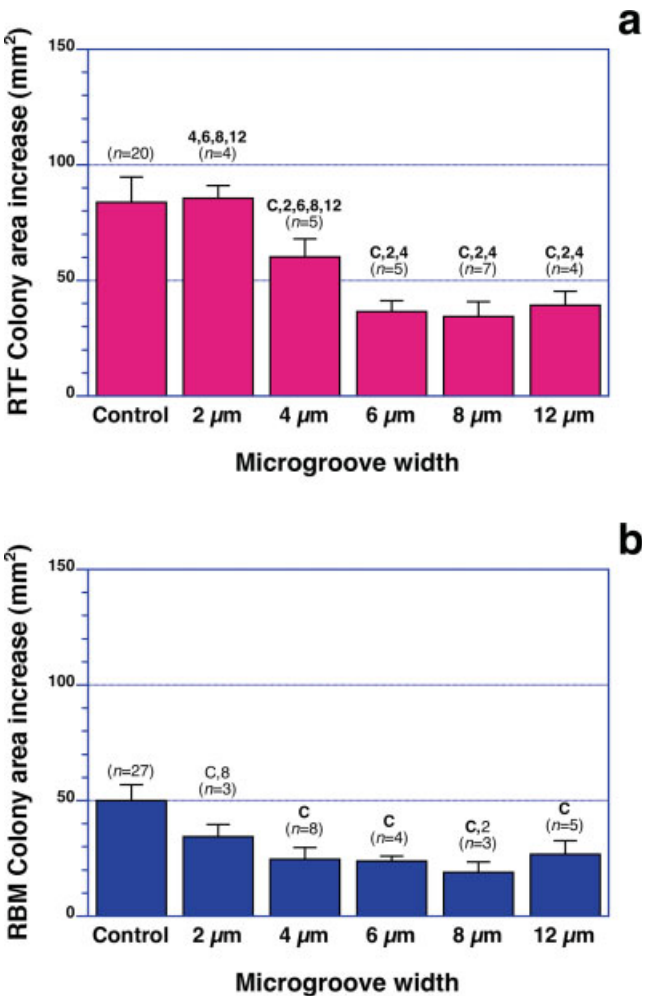

Figure 11. Graphs comparing mean increases, between days 4 and 8, in the projected areas of RTF (a) and RBM (b) colonies grown on microgrooved and control substrates. [Color figure can be viewed in the online issue, which is available at www.interscience.wiley.com.]

Our results clearly demonstrate that substrate microgrooves cause contact guidance of connective tissue cells *in vitro*. The orientation of cells, their matrix protein products, and their underlying substrate features are strongly interrelated. Cell orientation has been shown to polarize cells and their axes of mitotic division[29,38] and directions of migration,[102] which presumably caused the elongated growth of our colonies. Moreover, cell orientation also determines the pattern of collagen synthesis by fibroblasts[103,104] and bone cells.[82,105–109] The orientation of matrix molecules is itself capable of determining the mitotic axis in HeLa cells.[110] Responses to growth factors[111] and production of nonmatrix molecules[112,113] are also altered in cells oriented by microgrooves.

Both RBM and RTF cells bridged the ridges between the 2-μm grooves, resulting in cells that were flatter, well spread, and more variably oriented than those grown on the 6-, 8-, and 12-μm grooves. Populations of RBM and RTF cells grown on 4-μm grooves consisted of cells that were flattened and well spread along with We observed appreciable width increases by colonies of RBM cells on the 2-μm grooves, and by RTF colonies on the 2- and 4-μm grooves. Additionally, RBM and RTF colonies grown on the 12 μm-grooves increased in width more than colonies grown on 6- and 8-μm grooves. This may have been a result of the dimensions of the microgrooves themselves. The larger microgrooves may have spread cells apart enough without permitting them to grow parallel to one another, thus appearing to widen the colony. Conversely, the 12 μm-grooves may be sufficiently larger than the cells to allow some degree of diagonal cell orientation, resulting in increased in colony width.

The increased lengths and decreased widths of RTF and RBM colonies grown on 4-, 6-, 8-, and 12-μm grooves significantly ($p \leq 0.01$) suppressed the overall growth of the colonies, as determined by colony area, when compared with controls. RBM colony growth on the 2-μm grooves was also significantly decreased ($p \leq 0.05$), but the growth of RTF colonies on the 2-μm grooves was equivalent to that of controls. The affect of the 2-μm grooves on colony area increase was presumably due to the greater colony width increases seen in these groups. Importantly, the suppression of cell growth differed between cell types in several ways. This offers the opportunity to design implant surfaces that differentially favor the growth one cell type over the other.[51,53]

Correlation with *in vivo* studies

The present results explain some of the observations that we have made of the *in vivo* effects of microgrooved surfaces on cells and tissues. Our results correlate well with our previous *in vivo* studies of titanium dioxide-coated polystyrene, titanium alloy, and commercially-pure titanium implants with controlled microgeometries.[37,47,51,53,106,114] Those studies demonstrated that surface microgrooves of similar sizes employed in the present study enhance bony integration and orient the local microstructure of attached bone. Light and electron microscopic observations suggested that those surfaces orientated the cells, which in turn produced similarly oriented matrix molecules (collagen fibers) and bone microstructures (trabeculae). Other investigators demonstrated that surface roughening modifies bone cell responses to biological mediators and differentiation patterns.[54,55] Well-defined substrate features may organize these factors in directionally or spatially determined ways that contribute to the overall *in vivo* responses that we observed. Nontextured, grit-blasted, and polished surfaces did not induce the production of oriented fibrous matrix or bone.[48,49] These effects may be employed to orient the formation of interfacial tissues surrounding an implant to best accommodate the mechanical forces brought to bear on the tissue-implant interface. Similar design features may also be employed to control the migration of gingival epithelial cells on dental implants, resulting in improved stabilization and osseointegration of the implants.[37,51,53,115]

It is likely that surface texturing works on multiple levels to improve implant stability. Textured surfaces have larger surface areas than smooth surfaces, creating a quantitatively larger mechanical interface. Textured surfaces also promote adhesion of fibrin[41] and other, more permanent matrix components, and affect long-term interaction of cells at stable interfaces.[31,48,49] In the short term, the formation of fibrous tissue is impaired by textured interfaces, when compared with smooth interfaces.[37,47–49] Textured surfaces have the additional advantage of resisting colonization by fibroblastic and macrophagic cells that arrive early during wound healing and initiate the encapsulation of smooth substrates.[44,45] Textured surfaces may also promote the differentiation of the bone-forming cells that form the critical interface with implant surfaces. The overall effect is that of improved implant stabilization during osseous incorporation and after complete assimilation into the body.[13,37,51–53,115]

References

1. National Center for Heath Statistics. Number and rate for surgical and nonsurgical procedures, 2001. Atlanta: Center for Disease Control and Prevention; 2003.
2. Millenium Research Group. US markets for dental implants: Executive summary. Implant Dent 2003;12:108–111.

3. Cameron HU, Hu C, Vyamont D. Hinge total knee replacement revisited. Can J Surg 1997;40:278–283.
4. Sennerby L, Roos J. Surgical determinants of clinical success of osseointegrated oral implants: A review of the literature. Int J Prosthodont 1998;11:408–420.
5. Bauer TW, Schils J. The pathology of total joint arthroplasty. II. Mechanisms of implant failure. Skeletal Radiol 1999;28: 483–497.
6. Bauer TW, Schils J. The pathology of total joint arthroplasty. I. Mechanisms of implant fixation. Skeletal Radiol 1999;28: 423–432.
7. Salvi GE, Lang NP. Changing paradigms in implant dentistry. Crit Rev Oral Biol Med 2001;12:262–272.
8. Steigenga JT, al-Shammari KF, Nociti FH, Misch CE, Wang HL. Dental implant design and its relationship to long-term implant success. Implant Dent 2003;12:306–317.
9. Albrektsson T, Hansson HA, Ivarsson B. Interface analysis of titanium and zirconium bone implants. Biomaterials 1985;6:97–101.
10. Albrektsson T, Hansson HA. An ultrastructural characterization of the interface between bone and sputtered titanium or stainless steel surfaces. Biomaterials 1986;7:201–205.
11. Albrektsson T, Wennerberg A. Oral implant surfaces: Part 1–review focusing on topographic and chemical properties of different surfaces and in vivo responses to them. Int J Prosthodont 2004;17:536–543.
12. Albrektsson T, Wennerberg A. The impact of oral implants—Past and future, 1966–2042. J Can Dent Assoc 2005;71:327.
13. Buser D, Schenk RK, Steinemann S, Fiorellini JP, Fox CH, Stich H. Influence of surface characteristics on bone integration of titanium implants. A histomorphometric study in miniature pigs. J Biomed Mater Res 1991;25:889–902.
14. Haddad RJ Jr, Cook SD, Thomas KA. Biological fixation of porous-coated implants. J Bone Joint Surg Am 1987;69:1459–1466.
15. Linder L, Carlsson A, Marsal L, Bjursten LM, Branemark PI. Clinical aspects of osseointegration in joint replacement. A histological study of titanium implants. J Bone Joint Surg Br 1988;70:550–555.
16. Ricci JL, Gona AG, Alexander H. In vitro tendon cell growth rates on a synthetic fiber scaffold material and on standard culture plates. J Biomed Mater Res 1991;25:651–666.
17. Thomas KA, Cook SD. An evaluation of variables influencing implant fixation by direct bone apposition. J Biomed Mater Res 1985;19:875–901.
18. Thomas KA, Kay JF, Cook SD, Jarcho M. The effect of surface macrotexture and hydroxylapatite coating on the mechanical strengths and histologic profiles of titanium implant materials. J Biomed Mater Res 1987;21:1395–1414.
19. Schwartz Z, Nasazky E, Boyan BD. Surface microtopography regulates osteointegration: The role of implant surface microtopography in osteointegration. Alpha Omegan 2005;98:9–19.
20. Wennerberg A, Hallgren C, Johansson C, Danelli S. A histomorphometric evaluation of screw-shaped implants each prepared with two surface roughnesses. Clin Oral Implants Res 1998;9:11–19.
21. Zhao G, Schwartz Z, Wieland M, Rupp F, Geis-Gerstorfer J, Cochran DL, Boyan BD. High surface energy enhances cell response to titanium substrate microstructure. J Biomed Mater Res A 2005;74:49–58.
22. Zinger O, Zhao G, Schwartz Z, Simpson J, Wieland M, Landolt D, Boyan B. Differential regulation of osteoblasts by substrate microstructural features. Biomaterials 2005;26: 1837–1847.
23. Loesberg WA, Walboomers XF, van Loon JJ, Jansen JA. The effect of combined cyclic mechanical stretching and microgrooved surface topography on the behavior of fibroblasts. J Biomed Mater Res A 2005;75:723–732.
24. den Braber ET, de Ruijter JE, Jansen JA. The effect of a subcutaneous silicone rubber implant with shallow surface microgrooves on the surrounding tissues in rabbits. J Biomed Mater Res 1997;37:539–547.
25. Walboomers XF, Jansen JA. Microgrooved silicone subcutaneous implants in guinea pigs. Biomaterials 2000;21:629–636.
26. Chehroudi B, Gould TR, Brunette DM. Titanium-coated micromachined grooves of different dimensions affect epithelial and connective-tissue cells differently in vivo. J Biomed Mater Res 1990;24:1203–1219.
27. Brunette DM. Spreading and orientation of epithelial cells on grooved substrata. Exp Cell Res 1986;167:203–217.
28. Brunette DM. Fibroblasts on micromachined substrata orient hierarchically to grooves of different dimensions. Exp Cell Res 1986;164:11–26.
29. Brunette DM, Kenner GS, Gould TR. Grooved titanium surfaces orient growth and migration of cells from human gingival explants. J Dent Res 1983;62:1045–1048.
30. Clark P, Connolly P, Curtis AS, Dow JA, Wilkinson CD. Topographical control of cell behaviour. II. Multiple grooved substrata. Development 1990;108:635–644.
31. Curtis AS, Wilkinson CD, Crossan J, Broadley C, Darmani H, Johal KK, Jorgensen H, Monaghan W. An in vivo microfabricated scaffold for tendon repair. Eur Cell Mater 2005; 9:50–57; discussion 57.
32. Parker JA, Walboomers XF, Von den Hoff JW, Maltha JC, Jansen JA. The effect of bone anchoring and micro-grooves on the soft tissue reaction to implants. Biomaterials 2002;23:3887–3896.
33. Parker JA, Walboomers XF, Von den Hoff JW, Maltha JC, Jansen JA. Soft-tissue response to silicone and poly-L-lactic acid implants with a periodic or random surface micropattern. J Biomed Mater Res 2002;61:91–98.
34. Parker JA, Walboomers XF, Von Den Hoff JW, Maltha JC, Jansen JA. Soft tissue reaction to microgrooved poly-L-lactic acid implants loaded with transforming growth factor beta(3). Tissue Eng 2003;9:117–126.
35. Uttayarat P, Toworfe GK, Dietrich F, Lelkes PI, Composto RJ. Topographic guidance of endothelial cells on silicone surfaces with micro- to nanogrooves: Orientation of actin filaments and focal adhesions. J Biomed Mater Res A 2005;75:668–680.
36. Fitton JH, Dalton BA, Beumer G, Johnson G, Griesser HJ, Steele JG. Surface topography can interfere with epithelial tissue migration. J Biomed Mater Res 1998;42:245–257.
37. Ricci J, Charvet J, Frenkel S, Chang R, Nadkarni P, Turner J, Alexander H. Bone responses to laser microtextured surfaces. In: Davies J, editor. Bone Engineering. Toronto: em2; 2000. p 282–292.
38. Dalton BA, Walboomers XF, Dziegielewski M, Evans MD, Taylor S, Jansen JA, Steele JG. Modulation of epithelial tissue and cell migration by microgrooves. J Biomed Mater Res 2001;56:195–207.
39. Evans MD, McFarland GA, Taylor S, Walboomers XF. The response of healing corneal epithelium to grooved polymer surfaces. Biomaterials 2005;26:1703–1711.
40. Walboomers XF, Jansen JA. Effect of microtextured surfaces on the performance of percutaneous devices. J Biomed Mater Res A 2005;74:381–387.
41. Gemmel C, Park J. Initial blood interactions with endosseous implant materials. In: Davies J, editor. Bone Engineering. Toronto: em2; 2000. p 108–117.
42. Davies JE. Mechanisms of endosseous integration. Int J Prosthodont 1998;11:391–401.
43. Tan J, Saltzman WM. Topographical control of human neutrophil motility on micropatterned materials with various surface chemistry. Biomaterials 2002;23:3215–3225.

44. Tan J, Shen H, Carter KL, Saltzman WM. Controlling human polymorphonuclear leukocytes motility using microfabrication technology. J Biomed Mater Res 2000;51:694–702.
45. Tan J, Shen H, Saltzman WM. Micron-scale positioning of features influences the rate of polymorphonuclear leukocyte migration. Biophys J 2001;81:2569–2579.
46. Parker KK, Brock AL, Brangwynne C, Mannix RJ, Wang N, Ostuni E, Geisse NA, Adams JC, Whitesides GM, Ingber DE. Directional control of lamellipodia extension by constraining cell shape and orienting cell tractional forces. FASEB J 2002;16:1195–1204.
47. Frenkel SR, Simon J, Alexander H, Dennis M, Ricci JL. Osseointegration on metallic implant surfaces: Effects of microgeometry and growth factor treatment. J Biomed Mater Res 2002;63:706–713.
48. Frenkel SR, Alexander H, Dennis M, Ricci JL. Effects of microgeometry and growth factor treatment on osseointegration of metallic implant surfaces. Trans Orthop Res Soc 1999;22:891.
49. Frenkel SR, Simon J, Alexander H, Dennis M, Ricci JL. Osseointegration on metallic surfaces: Effects of microgeometry and growth factor treatment. Trans Soc Biomater 1998;21:66.
50. Chehroudi B, Gould TR, Brunette DM. The role of connective tissue in inhibiting epithelial downgrowth on titanium-coated percutaneous implants. J Biomed Mater Res 1992;26:493–515.
51. Alexander H, Ricci JL, Hrico JG. A mechanical basis for bone retention around dental implants. J Biomed Mater Res B Appl Biomater. 2007 23 April; PMID 17455277.
52. Buser D, Nydegger T, Oxland T, Cochran DL, Schenk RK, Hirt HP, Snetivy D, Nolte LP. Interface shear strength of titanium implants with a sandblasted and acid-etched surface: A biomechanical study in the maxilla of miniature pigs. J Biomed Mater Res 1999;45:75–83.
53. Weiner S, Zweig B, Simon J, Ricci JL. Advanced surface microtexturing techniques to enhance bone and soft tissue response to dental implllants. Implant Dent. Forthcoming.
54. Batzer R, Liu Y, Cochran DL, Szmuckler-Moncler S, Dean DD, Boyan BD, Schwartz Z. Prostaglandins mediate the effects of titanium surface roughness on MG63 osteoblast-like cells and alter cell responsiveness to 1 alpha,25-(OH)2D3. J Biomed Mater Res 1998;41:489–496.
55. Kieswetter K, Schwartz Z, Hummert TW, Cochran DL, Simpson J, Dean DD, Boyan BD. Surface roughness modulates the local production of growth factors and cytokines by osteoblast-like MG-63 cells. J Biomed Mater Res 1996;32:55–63.
56. Clark P, Connolly P, Curtis AS, Dow JA, Wilkinson CD. Cell guidance by ultrafine topography in vitro. J Cell Sci 1991;99(Part 1):73–77.
57. Ricci JL, Charvet J, Sealey R, Biton I, Green WS, Stuchin S, Alexander H. In vitro effects of surface roughness and controlled surface microgeometry on fibrous tissue cell colonization. Trans Soc Biomater 1995;18:115.
58. Ricci JL, Rose R, Charvet J, Alexander H, Naiman CS. Cell interaction with microtextured surfaces. Trans World Biomater Congr 1996;6:I–937.
59. Rovensky YA, Slavnaja IL, Vasiliev JM. Behaviour of fibroblast-like cells on grooved surfaces. Exp Cell Res 1971;65:193–201.
60. Kenar H, Kose GT, Hasirci V. Tissue engineering of bone on micropatterned biodegradable polyester films. Biomaterials 2006;27:885–895.
61. Lom B, Healy KE, Hockberger PE. A versatile technique for patterning biomolecules onto glass coverslips. J Neurosci Methods 1993;50:385–397.
62. Ito Y, Chen G, Imanishi Y. Micropatterned immobilization of epidermal growth factor to regulate cell function. Bioconjug Chem 1998;9:277–282.
63. Ozawa N, Yao T. Micropattern formation of apatite by combination of a biomimetic process and transcription of resist pattern. J Biomed Mater Res 2002;62:579–586.
64. Whitesides GM, Ostuni E, Takayama S, Jiang X, Ingber DE. Soft lithography in biology and biochemistry. Annu Rev Biomed Eng 2001;3:335–373.
65. Singhvi R, Kumar A, Lopez GP, Stephanopoulos GN, Wang DI, Whitesides GM, Ingber DE. Engineering cell shape and function. Science 1994;264:696–698.
66. Bhatia SN, Yarmush ML, Toner M. Controlling cell interactions by micropatterning in co-cultures: Hepatocytes and 3T3 fibroblasts. J Biomed Mater Res 1997;34:189–199.
67. Chen CS, Mrksich M, Huang S, Whitesides GM, Ingber DE. Geometric control of cell life and death. Science 1997;276:1425–1428.
68. Mrksich M, Dike LE, Tien J, Ingber DE, Whitesides GM. Using microcontact printing to pattern the attachment of mammalian cells to self-assembled monolayers of alkanethiolates on transparent films of gold and silver. Exp Cell Res 1997;235:305–313.
69. McClary KB, Grainger DW. RhoA-induced changes in fibroblasts cultured on organic monolayers. Biomaterials 1999;20:2435–2446.
70. Saneinejad S, Shoichet MS. Patterned glass surfaces direct cell adhesion and process outgrowth of primary neurons of the central nervous system. J Biomed Mater Res 1998;42: 13–19.
71. Saneinejad S, Shoichet MS. Patterned poly(chlorotrifluoroethylene) guides primary nerve cell adhesion and neurite outgrowth. J Biomed Mater Res 2000;50:465–474.
72. Deutsch J, Motlagh D, Russell B, Desai TA. Fabrication of microtextured membranes for cardiac myocyte attachment and orientation. J Biomed Mater Res 2000;53:267–275.
73. McDevitt TC, Angello JC, Whitney ML, Reinecke H, Hauschka SD, Murry CE, Stayton PS. In vitro generation of differentiated cardiac myofibers on micropatterned laminin surfaces. J Biomed Mater Res 2002;60:472–479.
74. Goessl A, Bowen-Pope DF, Hoffman AS. Control of shape and size of vascular smooth muscle cells in vitro by plasma lithography. J Biomed Mater Res 2001;57:15–24.
75. van Kooten TG, Whitesides JF, von Recum A. Influence of silicone (PDMS) surface texture on human skin fibroblast proliferation as determined by cell cycle analysis. J Biomed Mater Res 1998;43:1–14.
76. Ricci JL, Alexander H, Howard C. The influence of surface microgeometry on fibroblast colonization of synthetic surfaces. In: Cima LG, Ron ES, editors. Tissue-Inducing Biomaterials. Pittsburg: Materials Research Society; 1992. p 221–229.
77. Ricci JL, Charvet J, Chang R, Alexander H. Influence of surface microgeometry on in vitro cell growth and migration. In: Sudarshan TS, Ishizaki K, Takata M, Kamata K, editors. Surface Modification Technologies VII. London: The Institute of Materials; 1994. p 491–508.
78. Grew JC, Frenkel SR, Goldwyn E, Herman T, Ricci JL. Cytological characterization of 3T3 fibroblasts cultured on micropatterned substrates. Trans Soc Biomater 1998;21:40.
79. Grew JC, Ricci JL, Teitelbaum A-H, Charvet L. Effects of surface microgeometry on fibroblast shape and cytoskeleton. Trans Soc Biomater 1997;20:32.
80. den Braber ET, Jansen HV, de Boer MJ, Croes HJ, Elwenspoek M, Ginsel LA, Jansen JA. Scanning electron microscopic, transmission electron microscopic, and confocal laser scanning microscopic observation of fibroblasts cultured on microgrooved surfaces of bulk titanium substrata. J Biomed Mater Res 1998;40:425–433.
81. Walboomers XF, Croes HJ, Ginsel LA, Jansen JA. Contact guidance of rat fibroblasts on various implant materials. J Biomed Mater Res 1999;47:204–212.

82. Perizzolo D, Lacefield WR, Brunette DM. Interaction between topography and coating in the formation of bone nodules in culture for hydroxyapatite- and titanium-coated micromachined surfaces. J Biomed Mater Res 2001;56:494–503.
83. Anselme K, Bigerelle M, Noel B, Iost A, Hardouin P. Effect of grooved titanium substratum on human osteoblastic cell growth. J Biomed Mater Res 2002;60:529–540.
84. Chehroudi B, Brunette DM. Effects of surface topography on cell behavior. In: Donald DJT, editor. Encyclopedic Handbook of Biomaterials and Bioengineering. New York: Marcel Decker; 1995. p 813–842.
85. Grew JC, Ricci JL, Alexander H. Connective-tissue responses to defined biomaterial surfaces: Part II. Behavior of rat and mouse fibroblasts cultured on microgrooved substrates. J Biomed Mater Res. Forthcoming.
86. Lu X, Leng Y. Quantitative analysis of osteoblast behavior on microgrooved hydroxyapatite and titanium substrata. J Biomed Mater Res A 2003;66:677–687.
87. Ricci JL, Alexander H. In-vitro tendon cell growth on synthetic fiber implant materials: Biological implications. Bull Hosp Jt Dis Orthop Inst 1990;50:126–138.
88. Ricci JL, Gona AG, Alexander H, Parsons JR. Morphological characteristics of tendon cells cultured on synthetic fibers. J Biomed Mater Res 1984;18:1073–1087.
89. Schakenraad JM, Busscher HJ, Wildevuur CR, Arends J. The influence of substratum surface free energy on growth and spreading of human fibroblasts in the presence and absence of serum proteins. J Biomed Mater Res 1986;20:773–784.
90. van der Valk P, van Pelt AW, Busscher HJ, de Jong HP, Wildevuur CR, Arends J. Interaction of fibroblasts and polymer surfaces: Relationship between surface free energy and fibroblast spreading. J Biomed Mater Res 1983;17:807–817.
91. Horbett TA, Schway MB. Correlations between mouse 3T3 cell spreading and serum fibronectin adsorption on glass and hydroxyethylmethacrylate-ethylmethacrylate copolymers. J Biomed Mater Res 1988;22:763–793.
92. van Wachem PB, Mallens BW, Dekker A, Beugeling T, Feijen J, Bantjes A, Detmers JP, van Aken WG. Adsorption of fibronectin derived from serum and from human endothelial cells onto tissue culture polystyrene. J Biomed Mater Res 1987;21:1317–1327.
93. van Wachem PB, Vreriks CM, Beugeling T, Feijen J, Bantjes A, Detmers JP, van Aken WG. The influence of protein adsorption on interactions of cultured human endothelial cells with polymers. J Biomed Mater Res 1987;21:701–718.
94. Lenk TJ, Ratner BD, Gendreau RM, Chittur KK. IR spectral changes of bovine serum albumin upon surface adsorption. J Biomed Mater Res 1989;23:549–569.
95. Miller KM, Anderson JM. Human monocyte/macrophage activation and interleukin 1 generation by biomedical polymers. J Biomed Mater Res 1988;22:713–731.
96. Maniatopoulos C, Sodek J, Melcher AH. Bone formation in vitro by stromal cells obtained from bone marrow of young adult rats. Cell Tissue Res 1988;254:317–330.
97. Keller JC, Stanford CM, Wightman JP, Draughn RA, Zaharias R. Characterizations of titanium implant surfaces. III. J Biomed Mater Res 1994;28:939–946.
98. Healy KE, Ducheyne P. A physical model for the titanium-tissue interface. ASAIO Trans 1991;37:M150–M151.
99. Healy KE, Ducheyne P. Hydration and preferential molecular adsorption on titanium in vitro. Biomaterials 1992;13: 553–561.
100. Krause A, Cowles EA, Gronowicz G. Integrin-mediated signaling in osteoblasts on titanium implant materials. J Biomed Mater Res 2000;52:738–747.
101. Duval JL, Letort M, Sigot-Luizard MF. Comparative assessment of cell/substratum static adhesion using an in vitro organ culture method and computerized analysis system. Biomaterials 1988;9:155–161.
102. Diehl KA, Foley JD, Nealey PF, Murphy CJ. Nanoscale topography modulates corneal epithelial cell migration. J Biomed Mater Res A 2005;75:603–611.
103. Glass-Brudzinski J, Perizzolo D, Brunette DM. Effects of substratum surface topography on the organization of cells and collagen fibers in collagen gel cultures. J Biomed Mater Res 2002;61:608–618.
104. Yoshinari M, Matsuzaka K, Inoue T, Oda Y, Shimono M. Effects of multigrooved surfaces on fibroblast behavior. J Biomed Mater Res A 2003;65:359–368.
105. Khakbaznejad A, Chehroudi B, Brunette DM. Effects of titanium-coated micromachined grooved substrata on orienting layers of osteoblast-like cells and collagen fibers in culture. J Biomed Mater Res A 2004;70:206–218.
106. Soboyejo WO, Nemetski B, Allameh S, Marcantonio N, Mercer C, Ricci J. Interactions between MC3T3-E1 cells and textured Ti6Al4V surfaces. J Biomed Mater Res 2002;62:56–72.
107. Wang N, Ostuni E, Whitesides GM, Ingber DE. Micropatterning tractional forces in living cells. Cell Motil Cytoskeleton 2002;52:97–106.
108. Matsuzaka K, Yoshinari M, Shimono M, Inoue T. Effects of multigrooved surfaces on osteoblast-like cells in vitro: Scanning electron microscopic observation and mRNA expression of osteopontin and osteocalcin. J Biomed Mater Res A 2004;68:227–234.
109. Wang JH, Jia F, Gilbert TW, Woo SL. Cell orientation determines the alignment of cell-produced collagenous matrix. J Biomech 2003;36:97–102.
110. Thery M, Racine V, Pepin A, Piel M, Chen Y, Sibarita JB, Bornens M. The extracellular matrix guides the orientation of the cell division axis. Nat Cell Biol 2005;7:947–953.
111. Walboomers XF, Dalton BA, Evans MD, Steele JG, Jansen JA. Transforming growth factor-beta 1, 2, and 3 can inhibit epithelial tissue outgrowth on smooth and microgrooved substrates. J Biomed Mater Res 2002;60:445–451.
112. Hong HL, Brunette DM. Effect of cell shape on proteinase secretion by epithelial cells. J Cell Sci 1987;87(Part 2):259–267.
113. Matsuzaka K, Walboomers XF, Yoshinari M, Inoue T, Jansen JA. The attachment and growth behavior of osteoblast-like cells on microtextured surfaces. Biomaterials 2003;24:2711–2719.
114. Al-Habbab R, Weiner M, Bromage T, Ricci JL, Alexander H. Soft tissue response to laser-microtextured transcutaneous implants in a rabbit model. Trans Soc Biomater 2005;28:123.
115. Wennerberg A, Albrektsson T, Andersson B, Krol JJ. A histomorphometric and removal torque study of screw-shaped titanium implants with three different surface topographies. Clin Oral Implants Res 1995;6:24–30.